This article was downloaded by: [Renmin University of China]
On: 13 October 2013, At: 10:28
Publisher: Taylor & Francis
Informa Ltd Registered in England and Wales Registered Number: 1072954 Registered office: Mortimer House, 37-41 Mortimer Street, London W1T 3JH, UK

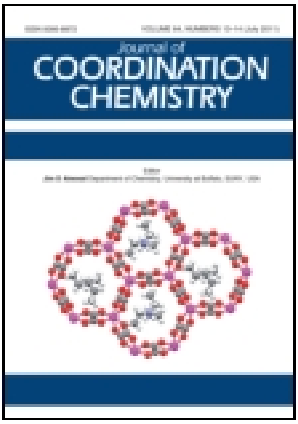

Journal of Coordination Chemistry
Publication details, including instructions for authors and subscription information:
http://www.tandfonline.com/loi/gcoo20

Structural aspects and solution behavior of metallosupramolecular compound of Fe^{III} ion obtained by proton transfer

H. Eshtiagh-Hosseini [a] , M. Mirzaei [a] , Z. Yousefi [a] , H. Puschmann [b] , A. Shokrollahi [c] & R. Aghaei [c]

[a] Department of Chemistry , Ferdowsi University of Mashhad , 917791436 Mashhad, Iran

[b] Department of Chemistry , Durham University , Durham DH1 3LE, UK

[c] Department of Chemistry , Yasouj University , Yasouj, Iran

Published online: 14 Nov 2011.

To cite this article: H. Eshtiagh-Hosseini , M. Mirzaei , Z. Yousefi , H. Puschmann , A. Shokrollahi & R. Aghaei (2011) Structural aspects and solution behavior of metallosupramolecular compound of Fe^{III} ion obtained by proton transfer, Journal of Coordination Chemistry, 64:22, 3969-3979, DOI: 10.1080/00958972.2011.634907

To link to this article: http://dx.doi.org/10.1080/00958972.2011.634907

PLEASE SCROLL DOWN FOR ARTICLE

Taylor & Francis makes every effort to ensure the accuracy of all the information (the “Content”) contained in the publications on our platform. However, Taylor & Francis, our agents, and our licensors make no representations or warranties whatsoever as to the accuracy, completeness, or suitability for any purpose of the Content. Any opinions and views expressed in this publication are the opinions and views of the authors, and are not the views of or endorsed by Taylor & Francis. The accuracy of the Content should not be relied upon and should be independently verified with primary sources of information. Taylor and Francis shall not be liable for any losses, actions, claims, proceedings, demands, costs, expenses, damages, and other liabilities whatsoever or howsoever caused arising directly or indirectly in connection with, in relation to or arising out of the use of the Content.

This article may be used for research, teaching, and private study purposes. Any substantial or systematic reproduction, redistribution, reselling, loan, sub-licensing,

Journal of Coordination Chemistry
Vol. 64, No. 22, 20 November 2011, 3969–3979

Structural aspects and solution behavior of metallosupramolecular compound of Fe^{III} ion obtained by proton transfer

H. ESHTIAGH-HOSSEINI†, M. MIRZAEI*†, Z. YOUSEFI†,
H. PUSCHMANN‡, A. SHOKROLLAHI§ and R. AGHAEI§

†Department of Chemistry, Ferdowsi University of Mashhad, 917791436 Mashhad, Iran
‡Department of Chemistry, Durham University, Durham DH1 3LE, UK
§Department of Chemistry, Yasouj University, Yasouj, Iran

(*Received 13 June 2011; in final form 14 October 2011*)

A supramolecular coordination compound of Fe^{III} containing pyridine-2,6-dicarboxylic acid ($pydcH_2$) and 2-aminopyrimidine (2-apym), $(2\text{-apymH})[Fe(pydc)_2]\cdot 2H_2O$ (**1**), was synthesized at normal conditions and characterized by elemental analysis, FTIR and UV spectroscopic methods, and X-ray crystallography. The crystallographic data of the compound show that it crystallizes in monoclinic lattice with space group $P2_1/c$. The constituent fragments of the compound were connected to each other by diverse intermolecular interactions such as hydrogen-bonding, π–π stacking, and ion pairing forming a supramolecular system. The solution studies show that there exist molecular aggregations in the solution compared with solid state. In the solution, ternary species are negligible but binary species such as ML_2 and ML_2H are present (L is referred to $pydcH_2$ moiety).

Keywords: Iron; Pyridine-2,6-dicarboxylic acid; 2-Aminopyrimidine; Supramolecular chemistry; Solution studies

1. Introduction

Metallosupramolecular chemistry attracts interest for potential applications in catalysis, sorption, photochemistry, magnetism, etc. A metallosupramolecular compound (MSC) is formed with interaction between organic molecules and metals. It is possible to construct a desired MSC by controlling factors, such as organic ligand, counter ion, solvent, and method of synthesis [1].

A variety of MSC have been constructed with pyridinedicarboxylic acid derivatives such as 2,3-, 2,4-, 2,5-, 2,6-dicarboxylic acid. Among them pyridine-2,6-dicarboxylic acid has been attracted some attention because of various coordination modes and biological activities of it.

Another factor affecting MSC architectures is counter ions. Organic moieties with particular functional groups are also important in construction of MSCs, playing

---

*Corresponding author. Email: mirzaeesh@um.ac.ir

Journal of Coordination Chemistry
ISSN 0095-8972 print/ISSN 1029-0389 online
http://dx.doi.org/10.1080/00958972.2011.634907

three essential roles in formation of these compounds, as ligand, neutral, or charged non-bonded moiety. To show these roles within different starting materials herein, we applied 2-aminopyrimidine (for short 2-apym). 2-apym as hydrogen bond donor and acceptor is a good candidate for the synthesis of new supramolecular compounds, in which 2-apym may play a role in construction of crystalline lattice by diverse intermolecular interactions [4–6].

In this article, we construct an MSC of Fe^{III} with $pydcH_2$ and 2-apymH as ligands, $(2\text{-apymH})[Fe(pydc)_2] \cdot 2H_2O$ (**1**). The compound was characterized with elemental analysis, FTIR and UV spectroscopic methods, and X-ray crystallography. The solution properties of the compound were determined to develop better understanding of the intermolecular interactions of the compound.

2. Experimental

2.1. *General methods and materials*

All chemicals were purchased from Merck Company and used without purification. Infrared spectra were recorded on a Bomem B-154 Fourier transform using KBr discs. Elemental analysis was performed on a Thermo Finnigan Flash-1112EA microanalyzer. X-ray data were obtained with an Oxford Diffraction Gemini Diffractometer. The melting point was determined using an Electro thermal IA-9100 apparatus and are uncorrected. UV spectra were obtained on an Agilent 8453 single beam photodiode array spectrometer. For potentiometric pH titration, a Model 794 Metrohm Basic Titrino was attached to a combined glass-calomel electrode mounted in an air-protected, sealed, thermostated jacketed cell maintained at $25.0 \pm 0.1^\circ C$ by circulating water from a constant-temperature bath with a Fisherbrand model FBH604, LAUDA, Germany, equipped with a stirrer and a 10,000-mL-capacity Metrohm piston burette. The pH meter-electrode system was calibrated to read $-\log[H^+]$. The procedure is described in references [7–9]. The concentrations of 2-apym and $pydcH_2$ were $2.50 \times 10^{-3}\,mol\,L^{-1}$ for the potentiometric pH titrations of $pydcH_2$, 2-apym and $pydcH_2 + 2$-apym, in the absence and presence of Fe^{3+} $1.25 \times 10^{-3}\,mol\,L^{-1}$. A standard carbonate-free NaOH solution ($0.102\,mol\,L^{-1}$) was used in all titrations. The ionic strength was adjusted to $0.1\,mol\,L^{-1}$ with $NaNO_3$. Before an experimental point (pH) was measured, sufficient time was allowed for establishment of equilibrium. Ligand protonation constants and stability constants of proton transfer and their metal complexes were evaluated using the BEST program described by Martell and Motekaitis [10]. The value of $K_w = [H^+]\,[OH^-]$ used in the calculations was according to our previous work [7–9].

2.2. *Synthesis of $(2\text{-apymH})[Fe(pydc)_2] \cdot 2H_2O$ (1)*

A solution of $Fe(NO_3)_3 \cdot 9H_2O$ (0.35 g, 1 mmol) in water (7 mL) was added to an aqueous solution of $pydcH_2$ (0.330 g, 2 mmol) and 2-apym (0.10 g, 1 mmol) in water (7 mL) with the molar ratio 1 : 2 : 1. The resulting solution was stirred at 70°C for 3 h. Light green crystals were isolated from the solution after 16 days by slow evaporation of solvent. Compound **1** was stable in air, soluble in water but insoluble in common organic solvents (yield 50% based on $Fe(NO_3)_3 \cdot 9H_2O$, m.p.: decomp. >300°). C.H.N analysis: Anal. Calcd for $C_{18}H_{12}FeN_5O_8$: C, 44.88; H, 2.51. Found: C, 43.72; H, 2.55. Selected FTIR bands (cm^{-1}): 3400(m), 3200(m), 3100(m), 1680(s), 1660(s), 1600(m), 1540(w), 1420(w), 1330(s), 1170(m), 1070(m), 1030(w), 920(m), 790(w), 770(m), 740(s), 680(m), 440(m). UV (H_2O, 10^{-5} M), λ_{max} (ε, 10^4): 220 (3.020), 270 (0.930), 277 (0.898).

3. Results and discussion

3.1. *Crystal structure of 1*

The crystal structure of **1** was determined with an Oxford Diffraction Gemini S Ultra diffractometer using Mo radiation. The structure was solved and refined using the Olex2 software package [11] in combination with SHELX [12]. The adopted numbering scheme of the non-hydrogen atoms along with anisotropic displacement ellipsoids of **1** are shown in figure 1. A summary of parameters for the data collection and refinements for **1** is given in table 1 and selected bond distances, angles, and torsion angles are given

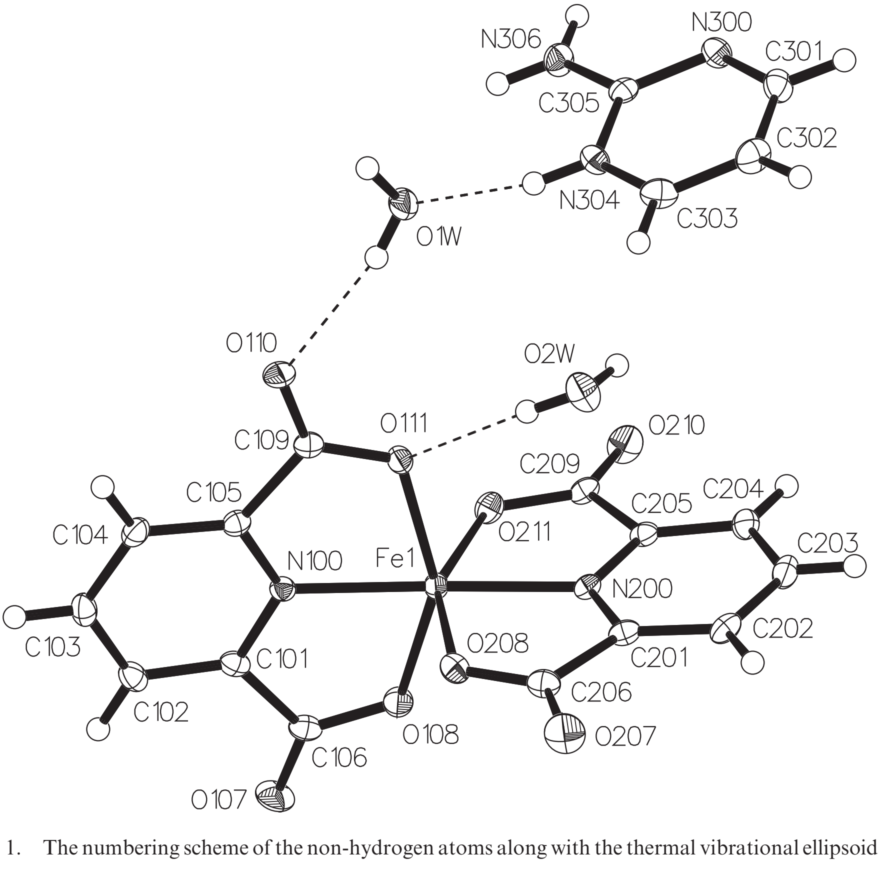

Figure 1. The numbering scheme of the non-hydrogen atoms along with the thermal vibrational ellipsoids of **1**.

Table 1. FTIR spectral data of **1**.

Empirical formula	$C_{18}H_{16}N_5FeO_{10}$
Formula weight ($g\,mol^{-1}$)	518.21
Temperature (K)	120.0
Crystal system	Monoclinic
Space group	$P2_1/c$
Unit cell dimensions (Å, °)	
a	9.4672(5)
b	18.0483(8)
c	11.9045(5)
β	95.504(5)
Volume ($Å^3$), Z	2024.71(16), 4
Calculated density ($Mg\,m^{-3}$)	1.700
Absorption coefficient (mm^{-1})	0.816
$F(000)$	1060
Crystal size (mm^3)	$0.575 \times 0.275 \times 0.167$
θ range for data collection (°)	2.48–27.00
Limiting indices	$-11 \leq h \leq 12$; $-22 \leq k \leq 22$; $15 \leq l \leq 15$
Reflections collected/unique	14,861/4386 [$R(\text{int}) = 0.0287$]
Data/restraint/parameters	4386/4/323
Completeness to $\theta = 25.75$ (%)	99.4
Goodness-of-fit on F^2	1.079
Final R indices [$I > 2\sigma(I)$]	$R_1 = 0.0290$, $wR_2 = 0.0782$
R indices (all data)	$R_1 = 0.0368$, $wR_2 = 0.0800$
Largest difference peak and hole ($e\,Å^{-3}$)	0.320 and −0.317

Table 2. Crystal data and structure refinement for **1**.

Fe1–O108	1.9770(11)	Fe1–N100	2.0659(14)
Fe1–O208	2.0523(12)	Fe1–N200	2.0505(13)
Fe1–O111	2.0593(12)		
Fe1–O211	2.0077(13)		
N200–Fe1–N100	167.40(6)	O108–Fe1–N200	109.55(5)
O211–Fe1–N100	114.65(5)	O108–Fe1–O211	93.85(5)
O211–Fe1–N200	76.56(5)	O108–Fe1–O208	94.29(5)
O211–Fe1–O111	93.31(5)	O111–Fe1–N100	75.13(5)
O211–Fe1–O208	152.17(5)	O208–Fe1–N100	93.13(5)
O108–Fe1–O111	151.17(5)	O208–Fe1–O111	92.27(5)
O108–Fe1–N100	76.50(5)	N200–Fe1–O111	99.28(5)
N200–Fe1–O208	75.64(5)		
O111–Fe1–O208–C206	−99.58(11)	O111–Fe1–O211–C209	96.87(12)

Table 3. Selected bond lengths (Å) and angles (°) for **1**.

D–H···A	d(D–H)	d(H···A)	d(D···A)	D–H···A
O1W–H···N304	0.8804(13)	1.8281(13)	2.6801(18)	162.48(11)
O1W–H···O110	0.807(14)	2.058(15)	2.8497(17)	166.9(21)
O1W–H···O207	0.831(23)	1.876(23)	2.7018(19)	172.3(24)
N306–H···O208	0.8800(14)	2.2072(10)	3.0192(17)	153.27(10)
O2W–H···O110	0.836(21)	2.102(20)	2.9586(17)	172.2(20)
N306–H···O107	0.8796(15)	2.4520(13)	3.1448(19)	136.01(10)
O2W–H···O111	0.845(15)	2.178(17)	3.0060(17)	166.6(29)

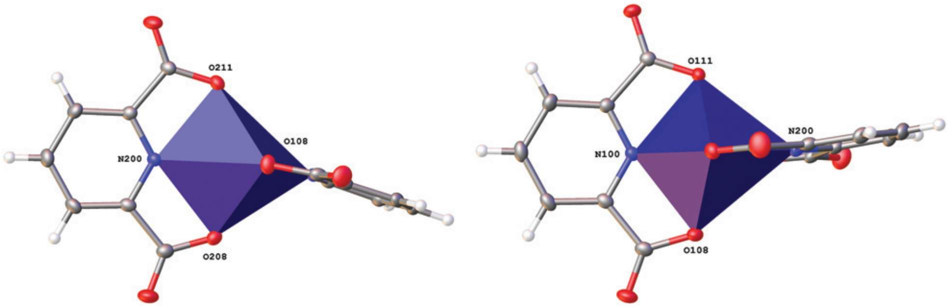

Figure 2. The anionic complex with perpendicular $(pydc)^{2-}$.

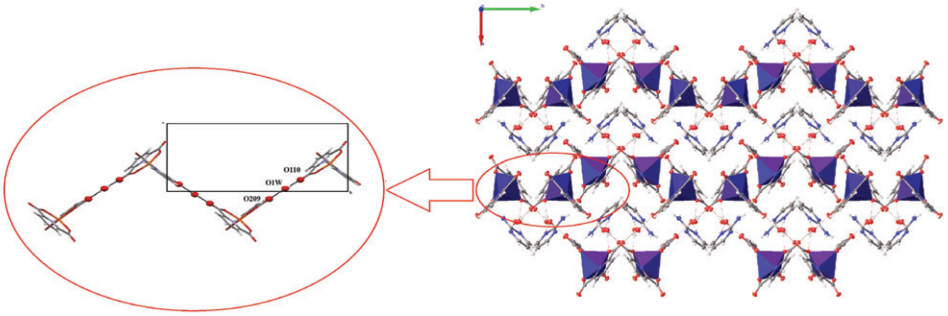

Figure 3. Packing diagram of **1** considering H-bond interactions in the *c*-direction.

in table 2. In addition, a list of hydrogen bonds is given in table 3. In the asymmetric unit, the molecular structure of **1** contains $[Fe(pydc)_2]^-$ with $(2\text{-apymH})^+$, and water in a 1 : 1 : 2 molar ratio, respectively. Based on molecular structure analysis, it is plausible that the coordination environment around Fe^{III} is mononuclear with a distorted octahedral geometry by two nitrogen atoms and four oxygen atoms of carboxylate of two perpendicular $(pydc)^{2-}$ fragments (figure 2). The volume of the distorted octahedron is 10.4592(40) Å^3. The bond distances of Fe–O and Fe–N lie at the normal range according to previous reports (table 2) [13a]. The monomeric unit of **1** along with O1W (O1W ··· O110, O1W ··· O207) aggregate along screw axes 2_1 in the *c*-direction, and this chain extends to the *ab*-plane by more hydrogen-bonding from 2-apymH and O2W (figure 3). As mentioned earlier, one effective factor on ultimate crystalline network is counter ions in MSCs. Several coordination compounds with Fe(III) and $pydcH_2$ have been prepared with different cationic moieties. Herein, we carried out a simple comparison between the packing diagrams for exploring the effect of counter-ion. Representative examples of the some packing motifs are presented in figure 4. These compounds include $(dmphenH)[Fe(pydc)_2]\cdot H_2O$ [13b] (**2**), $(2,2'\text{-bipyH})[Fe(pydc)_2]\cdot 3H_2O$ [14] (**3**), $(4,4'\text{-bipyH})[Fe(pydc)_2]\cdot 2H_2O$ [15] (**4**), $(bmmpaH)[Fe(pydc)_2](EtOH)_{0.8}(H_2O)_{0.2}$ [16] (**5**) and $(2\text{-apymH})[Cr(pydc)_2]\cdot 2H_2O$ [17] (**6**) (dmphen = 2,9-dimethyl-1.10-phenanthroline, 2,2′-bipy = 2,2′-bipyridine, 4,4′-bipy = 4,4′-bipyridine, bmmpa = 5-bromo-6-methyl-2-morpholinepyrimidine-4-amine).

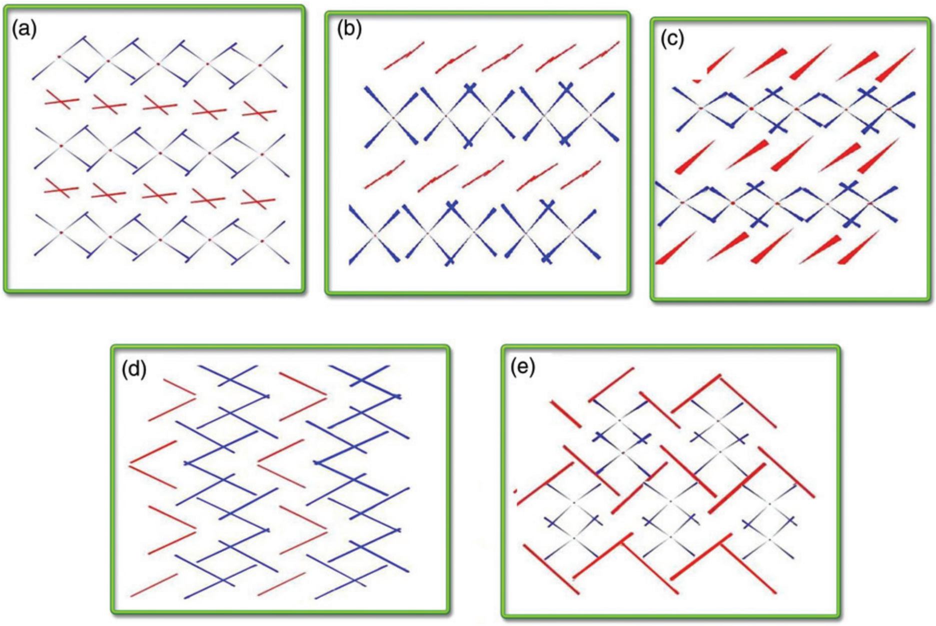

Figure 4. Schematic representation of packing diagrams of compounds related to (a) **4**; (b) **3**; (c) **5**; (d) **1,** and (e) **2**, respectively. The red and blue objects refer to counter-cations and anionic complexes, respectively.

There are π–π interactions between dmphen and one $(pydc)^{2-}$ in **2**; two-membered water clusters also exist. There are also three- and six-membered water clusters in **4** and **3**, respectively, which can play the role of glue. Every water cluster is connected to an anionic complex in **3**. As figure 4 shows, the packing diagrams due to **3**, **4**, and **5** are similar in the *c*-direction, and **1** and **6** are isostructural (the packing diagram of **6** is exactly similar to **1**, so it is not necessary).

The value of dihedral angle of the two pyridine rings within **1** (~85.62(4)°) verify that they are not coplanar and are almost perpendicular to each other. For this reason, bond angles belonging to FeO_4 in the equatorial plane deviate from ideal octahedral. Similar behavior was reported in our recent work [16, 17].

3.2. *Optical absorption*

There are three bands at 220, 270, and 277 nm in the electronic absorption spectrum of **1**. Absorptions at 220 nm and 270 nm are attributed to $n \rightarrow \pi^*$ and $\pi \rightarrow \pi^*$, respectively [18]. As nitrogen of $(pydc)^{2-}$ is coordinated to metal, $n \rightarrow \pi^*$ may belong to pyrimidine [17].

3.3. *IR spectrum*

Characteristic frequencies from the FTIR spectrum of **1** are listed in table 4. The most definitive feature in the composite spectrum is the presence of strong asymmetric and symmetric carboxylate stretching frequencies at 1600 and 1330 cm^{-1}, respectively [16, 17]. C=O stretching frequency is about 1680 cm^{-1} [19]. Disappearance of a broad band

Table 4. Interatomic distances related to intermolecular hydrogen-bonding (2-apymH)[Fe(pydc)$_2$] · 2H$_2$O (**1**) (Å and °).

Wavenumber (cm^{-1})	Assignment
1680	C=O stretching vibration
1600	Asymmetric stretching vibration of carboxylate
1330	Symmetric stretching vibration of carboxylate
1425	C=C stretching vibration due to aromatic ring
1480	C=N stretching of $(pydc)^{2-}$
3100	C–H stretching vibration
740	O–C–O in plane bending vibration

Table 5. Overall and stepwise protonation constants of pydcH$_2$ and 2-apym and recognition constants of interaction between them at 25°C and $\mu = 0.1\,mol\,L^{-1}$ $NaNO_3$.

Stoichiometry							
2-apym	pydcH$_2$	*h*	$\log \beta$	Equilibrium quotient *K*	$\log K$	Max (%)	at pH
0	1	1	4.85	–	4.85	93.9	3.6
0	1	2	7.30	–	2.45	55.9	2
1	0	1	4.31	–	3.74	99.5	2
1	1	1	7.54	[2-apympydcH]/[2-apymH][pydc]	2.69	27.0	4.6

at 2500–3300 cm^{-1} due to carboxyl O–H stretch shows the acid moiety deprotonated completely [19]. The absorption at 1425 cm^{-1} is due to the C=C stretching vibration of the $(pydc)^{2-}$ ring and the band at 1480 cm^{-1} is attributed to the C=N stretching vibration of $(pydc)^{2-}$ [17]. The δ (O–C–O) in plane deformation vibration and the stretching frequency of pyrimidine ring were located at 740 cm^{-1} [20] and 920 cm^{-1} [21], respectively.

3.4. *Solution study*

In preliminary experiments, the fully protonated form of pydcH$_2$ (L) and 2-apym (Q) were titrated with a standard NaOH aqueous solution to obtain protonation constants as building blocks of the pydcH$_2$–2-apym adduct. The protonation constants of pydcH$_2$ [7, 8] and 2-apym were calculated by fitting the potentiometric pH data to the BEST program. The results are summarized in table 5. The $\log \beta$ values are in good agreement with those reported for 2-apym [22]. Evaluation of the equilibrium constants for reactions of pydcH$_2$ with 2-apym in different protonation forms was accomplished through comparison of the calculated and experimental pH profiles, obtained with both pydcH$_2$ and 2-apym present [7, 23, 24] (table 5). The corresponding species distribution diagrams for 2-apym and pydcH$_2$–2-apym are shown in figures 5(b) and 6. The most abundant proton-transfer species present at pH 4.6 (27.0%) is 2-apympydcH ($\log K = 2.46$). Thus, solution studies provide additional evidence of association between 2-apym and pydcH$_2$, supporting the evidence from the solid state studies. In order to determine the stoichiometry and stability of the Fe^{3+} complexes with pydcH$_2$–2-apym proton-transfer system in aqueous solution, the equilibrium

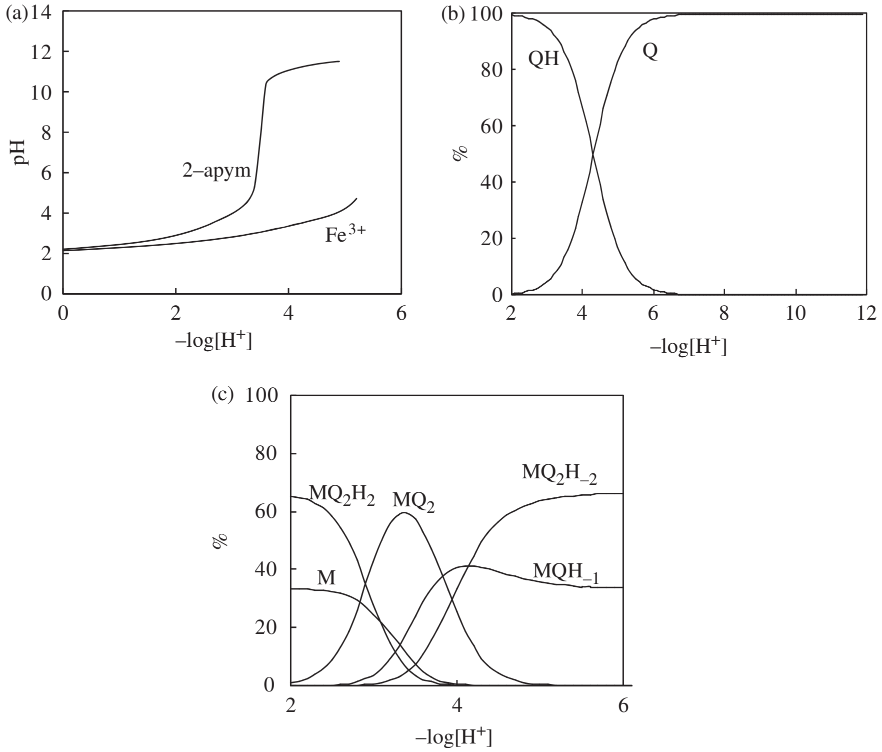

Figure 5. Potentiometric titration curve of pydcH$_2$ and 2-apym in the absence and presence of Fe^{3+} with NaOH 0.102 mol L^{-1} at 25°C and $\mu = 0.1$ mol L^{-1} NaNO$_3$ (a), distribution diagrams of 2-apym (Q) (b) and binary system 2-apym/Fe (c).

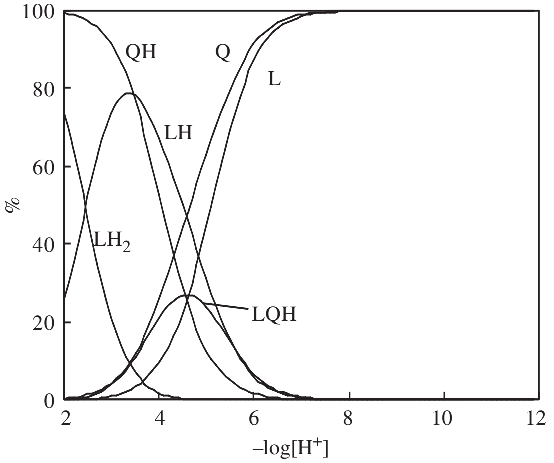

Figure 6. Distribution diagram of proton-transfer interaction between 2-apym (Q) and pydcH$_2$ (L).

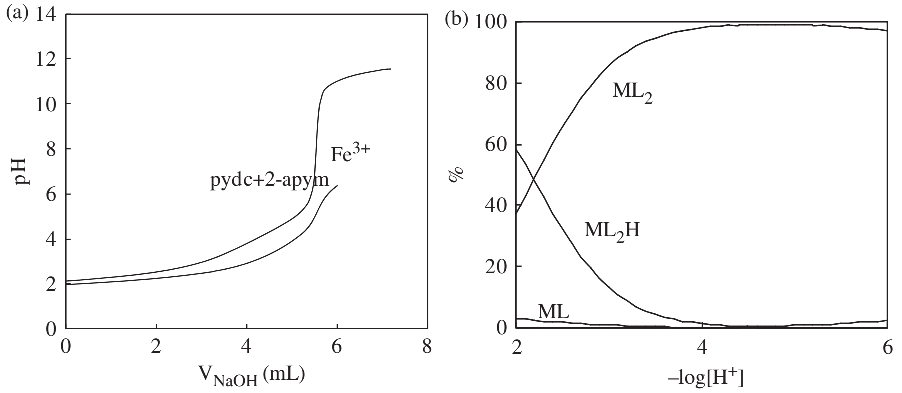

Figure 7. Potentiometric titration curves for pydcH$_2^{+2}$-apym in the absence and presence of Fe^{3+} with NaOH 0.102 mol L^{-1} at 25°C and $\mu = 0.1$ mol L^{-1} NaNO$_3$ (a), and distribution diagram of pydcH$_2$(L)/2-apym (Q)/Fe^{3+} ternary system (b).

Table 6. Overall stability constants of 2-apym/pydcH$_2$/Fe^{3+} binary and ternary systems at 25°C and $\mu = 0.1$ mol L^{-1} NaNO$_3$.

System	*m*	*l*	*q*	*h*	log *β*	Max (%)	at pH
2-apym–Fe	1	0	2	0	9.25	59.4	3.4
	1	0	2	2	15.07	65.4	2.0
	1	0	1	−2	−2.31	41.2	4.1
	1	0	2	−2	1.37	66.6	4.7 <
Fe–pydcH$_2$–2-apym	1	1	1	0	10.25	Negligible	–
	1	1	1	1	12.10	Negligible	–
	1	2	1	1	19.58	Negligible	–
	1	2	1	2	21.94	Negligible	–
	1	2	2	2	28.46	Negligible	–

potentiometric pH titration profiles of pydcH$_2$ [8], 2-apym and their 1 : 1 mixture were obtained in the absence and presence of the Fe^{3+} (figures 5a and 7a). In our previous publication [8] we reported relatively strong interaction between pydcH$_2$ and Fe^{3+}. As shown in figures 5(a) and 7(a) in the cases of 2-apym and pydcH$_2$–2-apym significant interactions were observed with Fe^{3+}. Similar results for 2-apym–M were reported for Mn^{2+}, Ni^{2+}, and Cu^{2+} [25]. The cumulative stability constants of M$_m$L$_l$Q$_q$H$_h$, complexes β_{mlqh}, are defined in our previous publications [7, 8]. There are M, L, Q, and H as metal ion, pydcH$_2$, 2-apym, and proton, respectively, and m, l, q, and h are the respective stoichiometric coefficients. The cumulative stability constants were evaluated by fitting the corresponding pH titration curves to the BEST program and the resulting values for the most likely complexed species in aqueous solutions are also included in table 6. The corresponding species distribution diagrams for pydcH$_2$ [8], 2-apym, and pydcH$_2$–2-apym in the presence of Fe^{3+} are shown in figures 5(c) and 7(b). The observed species and their corresponding stability constants of the pydcH$_2$–Fe system are given in our previous publication [8]. For 2-apym–Fe binary system as shown in table 6 and figure 5(c) most likely species are FeQ$_2$, FeQ$_2$H$_2$, FeQH$_{-2}$, and FeQ$_2$H$_{-2}$. In the case of pydcH$_2$–2-apym–Fe system, figure 7(b) and table 6, the ternary species are negligible but binary species such as ML_2 and ML_2H are abundant.

According to table 6, the interaction between Fe^{3+} and pydc in solution can be through tridentate pydc and very strong, and interaction between Fe^{3+} and 2-apym is very weak.

As $(pydc)^{2-}$ fully coordinate iron in $[Fe(pydc)_2]^-$, interaction between 2-apym by hydrogen-bonding is very weak or impossible. Therefore, the ternary species is not seen in solution and most abundant are Fe–$pydcH_2$ binary complexes.

4. Conclusion

In this article, we have characterized an MSC of Fe^{III} with $pydcH_2$ and 2-apym as counter cation and also studied solution behavior. The solution studies show that the aggregation is different than in solid state. The ternary species is not seen in solution and the most abundant species are Fe–$pydcH_2$ binary complexes.

Supplementary material

Crystallographic data for the title compound has been deposited with the Cambridge Crystallographic Data Centre, CCDC 761897 for **1**. Copies of the data can be obtained free of charge on application to the Director, CCDC, 12 Union Road, Cambridge CB2 1EZ, UK (Fax: int. code +(1223)336-033; E-mail for inquiry: fileserv@ccdc.cam.ac.uk; E-mail for deposition: deposit@ccdc.cam.ac.uk).

Acknowledgments

The authors thank to the Ferdowsi University of Mashhad for the financial support of this article.

References

[1] M. Mirzaei, H. Aghabozorg, H. Eshtiagh-Hosseini. *J. Iran. Chem. Soc.*, **8**, 580 (2011).

[2] (a) A.T. Ćolak, O.Z. Yesilel, O. Büyükgüngor. *Polyhedron*, **29**, 2127 (2010); (b) C. Qin, X.L. Wang, E.B. Wang, Z.M. Su. *Inorg. Chem.*, **44**, 7122 (2005); (c) H.L. Gao, C. Cheng, B. Ding, W. Shi, H.B. Song, P. Cheng, D.Z. Liao, S.P. Yan, Z.H. Jiang. *J. Mol. Struct.*, **738**, 105 (2005); (d) A.B. Lago, R. Carballo, E. Garcìa-Martínez, E.M. Vázquez-López. *Cryst. Growth Des.*, **11**, 59 (2011).

[3] (a) F.G. Gelalcha, B. Bitterlich, G. Anilkumar, M.K. Tse, M. Beller. *Angew. Chem. Int. Ed.*, **46**, 7293 (2007); (b) S. Liang, Z. Liu, N. Liu, C. Liu, X. Di, J. Zhang. *J. Coord. Chem.*, **63**, 3441 (2010); (c) J. Wang, F. He, X. Wang, L. Tian, Z. Li. *J. Coord. Chem.*, **64**, 2312 (2011); (d) D.-Y. Ma, W.-X. Wang, Y.-W. Li. *J. Coord. Chem.*, **63**, 448 (2010); (e) X. Hu, Y. Li, Y. Wang, W. Du, J. Guo. *J. Coord. Chem.*, **62**, 3438 (2009); (f) H. Eshtiagh-Hosseini, M. Mirzaei, E. Eydizadeh, Z. Yousefi, K. Molcanov. *Acta Cryst.*, **E67**, m1411 (2011).

[4] G.A. van Albada, I. Mutikainen, U. Turpeinen, J. Reedijk. *Polyhedron*, **23**, 993 (2004).

[5] Y.G. Huang, D.Q. Yuan, Y.Q. Gong, F.L. Jiang, M.C. Hong. *J. Mol. Struct.*, **872**, 99 (2008).

[6] H. Eshtiagh-Hosseini, Z. Yousefi, M. Mirzaei. *Acta Cryst.*, **E65**, o2816 (2009).

[7] A. Moghimi, S. Sheshmani, A. Shokrollahi, M. Shamsipur, G. Kickelbik, H. Aghabozorg. *Z. Anorg. Allg. Chem.*, **631**, 160 (2005).

[8] H. Aghabozorg, F. Ramezanipour, J. Soleimannejad, M.A. Sharif, A. Shokrollahi, M. Shamsipur, A. Moghimi, J. Attar Gharamaleki, V. Lippolis, A.J. Blake. *Polish J. Chem.*, **82**, 487 (2008).

[9] A. Shokrollahi, M. Ghaedi, H.R. Rajabi, M.S. Niband. *Spectrochim. Acta, Part A*, **71**, 655 (2008).

[10] E. Martell, R.J. Motekaitis. *Determination and Use of Stability Constants*, 2nd Edn, VCH, New York (1992).

[11] O.V. Dolomanov, L.B. Bourhis, R.J. Gildea, J.C. Howard, H. Puschmann. *J. Appl. Cryst.*, **42**, 339 (2009).

[12] G.M. Sheldrick. *Acta Cryst.*, **A64**, 112 (2008).

[13] (a) M. Tabatabaee, F. Abbasi, B.M. Kukovec, N. Nasirizadeh. *J. Coord. Chem.*, **64**, 1718 (2011); (b) H. Aghabozorg, E. Sadrkhanlou, J. Soleimannejad, H. Adams. *Acta Cryst.*, **E63**, m1760 (2007).

[14] Q.H. Zhao, M.S. Zhang, R.B. Fang. *Acta Cryst.*, **E61**, m2575 (2005).

[15] J. Soleimannejad, H. Aghabozorg, S. Sheshmani. *Acta Cryst.*, **E66**, m411 (2010).

[16] H. Eshtiagh-Hosseini, Z. Yousefi, M. Shafiee, M. Mirzaei. *J. Coord. Chem.*, **63**, 3187 (2010).

[17] (a) H. Eshtiagh-Hosseini, Z. Yousefi, M. Mirzaei, Y.G. Chen, S.A. Beyramabadi, A. Shokrollahi, R. Aghaei. *J. Mol. Struct.*, **973**, 1 (2010); (b) M. Mirzaei, H. Eshtiagh-Hosseini, V. Lippolis, H. Aghabozorg, D. Kordestani, A. Shokrollahi, R. Aghaei, A.J. Blake. *Inorg. Chim. Acta*, **370**, 141 (2011).

[18] L. Wasylina, E. Kucharska, Z. Weglinsky, A. Puszko. *Chem. Heterocycl. Compd.*, **35**, 186 (1999).

[19] F. Ramezanipour, H. Aghabozorg, A. Shokrollahi, M. Shamsipur, H. Stoeckli-Evans, J. Soleimannejad, S. Sheshmani. *J. Mol. Struct.*, **779**, 77 (2005).

[20] A.T. Çolak, O.Z. Yeşilel, T. Hökelek, E. Şahin. *Struct. Chem.*, **19**, 285 (2008).

[21] G. Ponticelli, A. Spanu. *Transition Met. Chem.*, **24**, 370 (1999).

[22] A. Albert, R. Goldacre, J. Phillips. *J. Chem. Soc.*, 2240 (1948).

[23] J.B. English, A.E. Martell, R.J. Motekaitis, I. Murase. *Inorg. Chim. Acta*, **258**, 183 (1997).

[24] M.A. Sharif, H. Aghabozorg, A. Shokrollahi, G. Kickelbick, A. Moghimi, M. Shamsipur. *Polish J. Chem.*, **80**, 847 (2006).

[25] S.A. Abdel-Latif, H.B. Hassib, Y.M. Issa. *Spectrochim. Acta, Part A*, **67**, 950 (2007).